TOWARDS DEVELOPMENT OF A TRACE ELEMENT SAMPLING SYSTEM: *IN SITU* PRE-CONCENTRATION USING A BI-DIRECTIONAL PUMP

A THESIS SUBMITTED TO
THE GLOBAL ENVIRONMENTAL SCIENCE
UNDERGRADUATE DIVISION IN PARTIAL FULFILLMENT
OF THE REQUIREMENTS FOR THE DEGREE OF

BACHELOR OF SCIENCE

IN

GLOBAL ENVIRONMENTAL SCIENCE

May 2016

By
Nathaniel Harmon

Thesis Advisors

Dr. Chris Measures
Dr. Mariko Hatta

We certify that we have read this thesis and that, in our opinion, it is satisfactory in scope and quality as a thesis for the degree of Bachelor of Science in Global Environmental Science.

THESIS ADVISORS

_____
Dr. Chris Measures
Department of Oceanography

_____
Dr. Mariko Hatta
Department of Oceanography

For James Harmon, Erica Duncan, and Kristen Harmon for all the love and patience.

ACKNOWLEDGEMENTS

ABSTRACT

A method to pre-concentrate iron (Fe) from seawater samples in the laboratory has been developed. The expectation is eventual deployment in unattended platforms in hard to access regions as well as to act as an alternative to the current rosette-based sampling system for trace elements. The system consists of a bi-directional pump (milliGAT), a holding coil, a multi-position selection valve, and external columns packed with a Toyopearl AF-Chelate-650$^{®}$ resin. From measurements of iron spiked water samples before and after pre-concentration on the resin, it was found that the iron present in the sample was successfully adsorbed on to the resin. The pre-concentration efficiency of the resin is 97.47% ± 0.82%, and the maximum capacity of the resin measured during experiments is 446.71 ± 3.76μmol Fe L^{-1}. A detection limit for the analytical method of 355pM Fe was obtained.

TABLE OF CONTENTS

LIST OF TABLES

LIST OF FIGURES

LIST OF ABBREVIATIONS

Iron ....(Fe)

Trace Metal ....(TM)

Particulate Iron ....(pFe)

Dissolved Iron ....(dFe)

Electron Transport Chain .... (ETC)

High Nutrient Low Chlorophyll .... (HNLC)

Trace Metal Clean .... (TMC)

Iron Concentration Before Pre-Concentration ....(Fe$_s$)

Iron Concentration After Pre-Concentration...(Fe$_f$)

Iron Concentration Pre-Concentrated on Resin ....(Fe$_a$)

8-hydroxyquinoline .... (8HQ)

N,*N*-dimethyl-*p*-phenylenediamine dihydrocloride ....(DPD)

1.0 INTRODUCTION

1.1 Introduction

The work described below represents the first stage of the development of a pre-concentration technique for trace element acquisition that can be adapted for use in currently hard to access regions. This stage of the development concerns iron (Fe) based pre-concentration on to a resin column in a laboratory environment. As the body of work included in this thesis concerns mainly Fe, it is first necessary to establish a base of knowledge surrounding Fe, its origins and distribution patterns, as well as the history of marine trace metal (TM) acquisition.

1.2 Fe Background

Fe constitutes ~32% of the mass of the Earth, but because of mass segregation during Earth's formation the majority is confined to the core; Fe composes 2.9-5% by weight of the crust, with 3.5% as a widely accepted average (Morgan & Anders, 1980; Jickells et al. 2001). Fe can exist in multiple oxidation states ranging from -2 to +6, with +2 (Fe(II)) and +3 (Fe(III)) being the most common (Street & Paytan, 2005). Fe(II) and Fe(III) exist at the surface of the Earth as either particulate (pFe) or dissolved (dFe), and can be found as inorganic forms or attached to organic ligands. The distinction between particulate and dissolved Fe is based upon filter size, with particulate usually being defined as >0.2um while dissolved is < 0.2um (Street & Paytan, 2005). It is of note that dissolved Fe is not necessarily present as free Fe, as the dissolved portion can include iron complexed with organic molecules, Fe-oxyhydroxide, and other colloidal particles

(Street & Paytan, 2005). For means of simplicity we assume dFe to be bioavailable Fe (Street & Paytan, 2005); this relationship is generally thought to be true and will suffice for the scope of this thesis.

Fe is a very important trace metal for primary production in oxygen-evolving organisms (Martin, et al. 1994). All photosynthetic organisms use Fe as part of an electron transport chain (ETC) during the light-dependent reactions taking place in the thylakoid membrane of the chloroplasts (Raven et al. 1999). The ETC utilizes the redox transformations between Fe(II) and Fe(III), to transfer photochemically excited electrons along an energy gradient. The energy released from the transfer of electrons down the ETC is used to reduce NADP to NADPH (Raven et al. 1999). Fe is also used by cyanobacteria in the nitrogenase enzyme that catalyzes nitrogen fixation (Georgiadis, et al. 1992).

As a result of the requirement for Fe in primary production and nitrogen fixation and its low concentration in the marine environment it can be the limiting nutrient in some environments. As early as 1844 it was documented that the addition of Fe to chlorophyll containing plants greatly improved their growth (Gris, 1844). Large areas of the open ocean, roughly 20%, have been found to have the macronutrients nitrogen (NO_3) and phosphorus (PO_4) left in the surface waters after the conclusion of the growing season (Martin, et al. 1994). These areas are know as High Nutrient Low Chlorophyll (HNLC) regions, and it was proposed that the disparity between macronutrient availability and primary production was due to Fe limitation, this was called the "Iron Limitation Hypothesis" (Martin, et al. 1994). Not until the 1980s and the advent of trace-metal clean sampling techniques (see below) was it possible to test the "Iron Limitation

Hypothesis" (Martin, et al. 1994). Trace metal clean sampling of HNLC areas revealed that they had Fe concentrations in the picomolar range, and addition of Fe to seawater incubations increased biomass production (Martin, et al. 1994, Sunda, et al. 1991).

The depletion of dFe at the surface of the ocean is a result of phytoplankton uptake (Martin & Gordon, 1988). Uptake of Fe is followed by vertical transport by the sinking flux of dead phytoplankton and detritus (Martin & Gordon, 1988). As the particles sink they decompose, utilizing oxygen to regenerate CO_2, NO_3, Fe, and other nutrients at depth (Martin & Gordon, 1988). The nutrients are eventually upwelled back to the surface. Dissolved Fe is scavenged continually from the subsurface waters depleting its concentration. Continued depletion results in an insufficient Fe concentration when this water is upwelled back to the surface ocean thus preventing the full uptake of the accompanying macronutrients (Martin & Gordon, 1988). Thus additional Fe needs to be added to the surface waters to permit full utilization of the upwelled macronutrients.

1.3 Fluvial Sources

The majority of Fe delivered to the ocean is via fluvial transport derived from the weathering of continental crust (Figure 1). Rivers transport ~37 x 10^{12} m^3 H_2O/yr to the ocean with an Fe load of ~13 Tmol (Street & Paytan, 2005; Fantle & DePaolo, 2004). At the surface of the Earth, the presence of O_2 in the atmosphere results in the oxidation of Fe to the Fe(III) oxidation state. Photochemical reduction by sunlight can produce a very low steady state concentration of dissolved Fe(II) in surface river water, however at pH's above ~5, in the presence of O_2, Fe(II) oxidizes rapidly to Fe(III) (Fantle & DePaolo,

2004). Dissolved Fe(III) released from the weathering of continental materials is highly

reactive and is quickly scavenged on the surface of particles as it travels down-river, and

in particular is affected by the chemical gradients and mixing processes in estuaries.

Flocculation in estuaries is the process in which fine suspended particles clump together

and settle out, and is a result of hydrolysis, complexation by organic ligands, which

ultimately make it mostly unavailable for biological use (Street & Paytan, 2005). This

results in only ~0.003 Tmol dFe, 0.02% of total riverine Fe, being delivered to near shore

communities (Figure 1; Fantle & DePaolo, 2004).
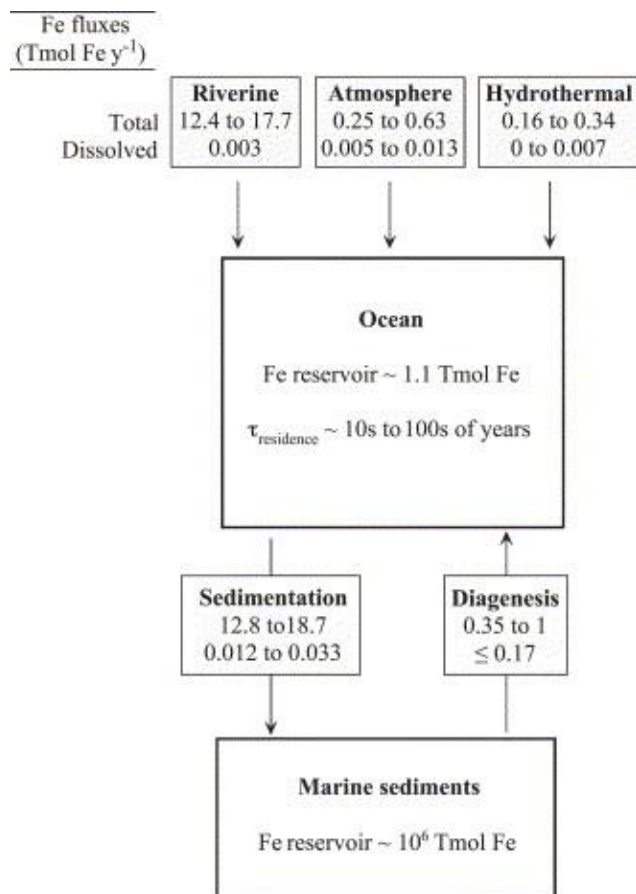

Figure 1: Global Oceanic Fe box model.

Figure 1: Simple box model depicting global average Fe fluxes in Tmol Fe yr^{-1} and reservoirs in Tmol Fe. Flux boxes show both total Fe flux (top) and dFe flux (bottom). (Fantle & DePaolo, 2004)

1.4 Eolian Sources

Despite being the most nutrient rich area of the ocean, coastal zones only account for 10% of the total oceanic area and 20% of the total oceanic primary production (Antoine et al. 1996). The remaining 80% of primary production takes place in the open ocean, which covers 90% of the oceanic area (Antoine et al. 1996). Because fluvial iron is rapidly scavenged near the coasts little makes it to the open ocean, requiring other sources. While the total Fe flux to the ocean is dominated by riverine transport, an equal, if not greater, amount of the dFe flux is delivered by atmospheric transport (Figure 1; Fantle & DePaolo, 2004). To understand how eolian dFe is delivered one must first look at the sources of atmospheric dust.

Atmospheric mineral dust, contains on average ~4% Fe by weight, is the result of a number of distinct processes: weathering, entrainment, and transport (Street & Paytan, 2005). The main sources of dust are the major arid regions of the globe: Central Asia, China, Australia, SW North America, South America, North Africa, and the Arabian Peninsula (Figure 2; Prospero et al. 2002). The areas mentioned have a commonality in that they, for the most part, are found in the mid-latitudes as well as being adjacent to highland regions (Mahowald et al. 2005). Equally important as low precipitation in the arid areas for atmospheric entrainment, is high precipitation in bordering highland areas. Just as fluvial Fe is sourced by weathering, atmospheric Fe is also the product weathering. Yearly precipitation cycles in highland regions adjacent to arid zones results in the weathering of rocks.

Figure 2: Global Mean Dust Entrainment
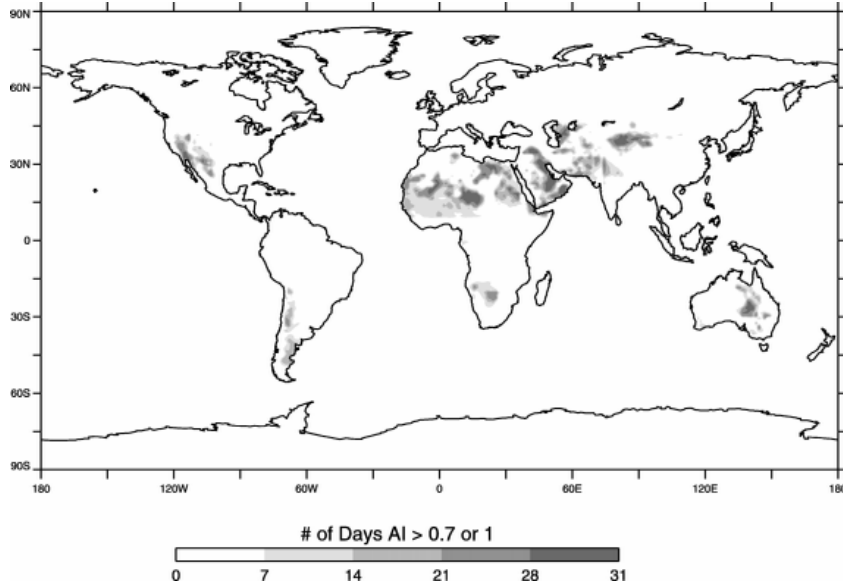
Figure 2: A representation of the monthly mean frequency of dust entrainment from all major dust sources globally, measured using Satellite spectrometry. (Prospero et al. 2002)

During the last glacial maximum small alluvial particles and dFe are transported from the parent rock to a drainage basin by glaciers and melt water, where the particles and dFe are deposited by gravity and when the transport medium is evaporated. Once the particles have been dehydrated, those at the micron scale become perfect candidates for deflation, atmospheric entrainment (Mahowald et al. 2005). In areas where glaciers form, such as the Himalayas, the weathering process is accelerated by the annual fluctuations in glacial volume. As the glaciers advance and retreat they physically and chemically weather large quantities of sediments, sediments that are flushed to outwash plains that can contribute to dust production (Sugden et al. 2009).

Results of a wind tunnel study suggest that the deflation of surface materials to form dust is proportional to the wind speed cubed (Duce et al. 1995). The proportional relationship means that particles in the 0.1-10μm size range will be deflated by near surface wind speeds (U_{10}) of 4–8 m s^{-1} (Sugden et al. 2009; Jickells et al. 2005). Particles

falling in the 0.1-10µm size range are acted upon by cohesive forces, they stick together and stay on the ground. As larger particles are blown by wind, however, saltation occurs. Saltation is a horizontal flux of relatively large grounded particles (>100µm) across a surface causing abrasion of smaller particles, with consequent weakening of cohesive forces. The weakening of cohesive forces from saltation results in a vertical flux, deflation (Mahowald et al. 2005).

While the whole of an arid basin is responsible for dust production, areas along the edges of the regions and dried out lakebeds provide the majority of dust (Mahowald et al. 2005). These areas are prone to large episodic dust events entraining huge volumes of material, in addition in regions bordering oceans daily sea breezes can provide a steady source of dust to the atmosphere. The total global aerosol flux has been estimated at ~1700 Tg yr^{-1} (Jickells et al. 2005). As the Fe content of dust reflects the composition of the parent material, ~3.5% Fe by weight the total Fe flux to the atmosphere from dust production is estimated at ~50-100 Tg yr^{-1} (Street & Paytan, 2005).

The residence time of the dust in the atmosphere is an important factor in determining the global distribution of the eolian material. The larger particles, >10µm, have very short residences times and are deposited close to their source primarily by gravitational settling or wet deposition from rain processes (Jickells et al. 2005). The residence time of the 0.1-10µm particle size range, ranges from hours to weeks in the atmosphere (Morales, C. 1986, Jickells et al. 2005). Because the residence time of dust in the atmosphere is much less than the inter-hemispheric mixing rate, 1-1.5yr, and as the main removal process is rain with the equator acting as a rain barrier, terrestrially derived dust is mainly deposited in the hemisphere in which it was created (Bowman & Cohen,

1997). Also, the majority of sources for dust production are located in the Northern

Hemisphere, such that there is a strong bias in deposition towards Northern Hemisphere

(Figure 3).

Figure 3: Average Dust Deposition
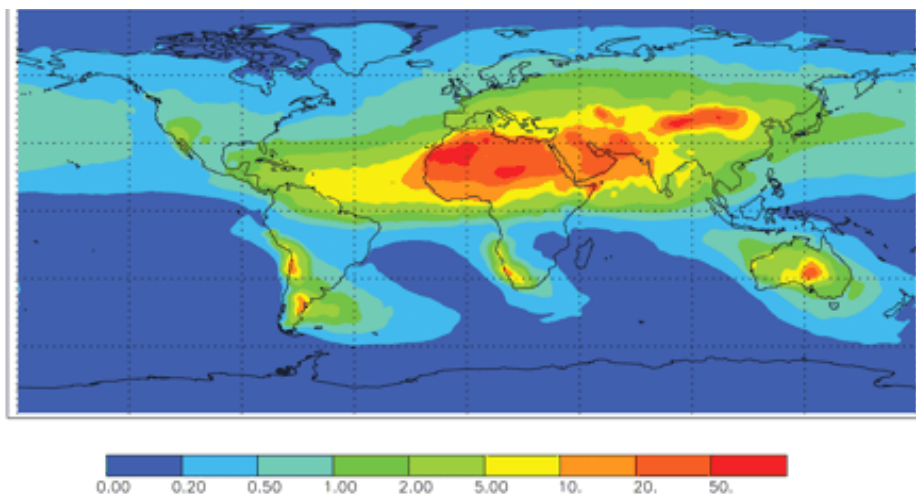
Figure 3: A composite of 3 models of Atmospheric Dust deposition measured in g m^{-2} yr^{-1}. Note the strong bias towards deposition in the northern hemisphere and how deposition follows the prevailing geostrophic winds (Jickells et al. 2005).

The final step in the delivery of eolian Fe to the surface ocean is deposition,

which can occur as dry or wet deposition (Street & Paytan, 2005). Wet deposition is the

deposition of particles by precipitation and is the result two separate processes, rainout

and washout. Washout occurs when particles are scavenged by the process of rain and

cloud formation as cloud condensation nuclei (Schlesinger & Bernhardt, 2013. p.74-75).

Rainout results when particles are scavenged below the cloud level by raindrops

(Schlesinger & Bernhardt, 2013. p.74-75). During the wet deposition process aerosol Fe

is exposed to more neutral pH conditions, first in rain then with introduction into the

seawater, pH ~8. The basic conditions cause Fe(II) to oxidize, and dFe to complex, this

lowers the dFe from ~10%, in the atmosphere, to ~0.3-6% (Street & Paytan, 2005). Wet

deposition makes up ~30% of deposition, the remaining ~70% of dust is deposited by dry deposition (Street & Paytan, 2005). Dry deposition is just the gravitational sedimentation of particles during dry periods. During dry deposition the acidic pH is preserved, and the dFe portion is maintained at ~10% (Schlesinger & Bernhardt, 2013. p.74-75). Both total global wet deposition and dry deposition are difficult to estimate; best estimates for both are ~20-320*10^{10} g yr^{-1} (Figure 1; Street & Paytan, 2005; Duce & Tindale, 1991).

The distance the mineral dust is transported is a function of its residence time which depends upon atmospheric conditions near the site of entrainment. A large portion of dust produced is transported towards the ocean (Jickells et al. 2005). Once over the ocean some dust is deposited near the coast, due to gravitational settling or washout from rain if the dust is below the marine boundary layer (Westphal et al. 1987). If strong winds are able to carry the dust above the marine boundary layer it can be transported 1000's of km at high altitudes (Measures et al. 2008). As noted many of the sites of dust production occur in the mid-latitudes corresponding to high winds flowing around large atmospheric highs (Figure 2). The dust is kept aloft above the marine boundary layer in a stable, dry atmospheric layer bordered by temperature inversions, once the dust reaches this layer it can then be transported around the gyres (Westphal et al. 1987). Dust settles out from the stable air layer based on its gravitational settling velocity, larger particles settle faster, down into the marine boundary layer where it is washed out by rain or falls into the ocean (Westphal et al. 1987). The mechanism described can account for much of the Fe deposited in the Pacific and Atlantic oceans.

During atmospheric transport, the dust is subjected to low pH conditions (pH 1-5.5) (Spokes & Jickells, 1995). The acidic conditions are a product of cloud formation

cycles (Duce & Tindale, 1991). During cloud formation the Fe in dust is exposed to acids

derived from sea salt ejecta (H_2SO_4) as well as from anthropogenic sources (Duce &

Tindale, 1991). Exposure to acidic conditions in clouds and the presence of UV radiation

results in photoreduction of particulate and colloidal Fe[III] to the more soluble Fe[II] by

means of the following reaction (Duce & Tindale, 1991).

(1) $$[Fe(OH)(H_2O)_5]^{2+} + H_2O$$

$$hv \rightarrow$$

$$[Fe(H_2O)_6]^{2+} + (OH)_{aq}$$

The reaction described above occurs spontaneously in the atmosphere, generating

substantial quantities of Fe[II], >55% (Duce & Tindale, 1991). An estimated ~10% of the

total Fe in the atmosphere is dFe (Duce & Tindale, 1991).

1.5 Hydrothermal Sources

Hydrothermal vent systems are located on or near tectonically active areas such as

hotspots and mid-ocean ridges (Figure 4). The vents release fluid consisting of seawater

that has percolated down through porous crustal rock and magma (Haase et al. 2007). In

the super-heated water that forms, Pyrite (FeS_2) is formed, which contributes stable

readily dissociable Fe(II) (Yucel et al. 2011). Until recently hydrothermal vents have

been relatively discounted as a globally important source of dFe as it was assumed that

the Fe in the vent water was scavenged immediately, but new research suggests that

hydrothermal vents are supplying dFe, that could be fueling an estimated 50 Pg C yr^{-1} of

primary production in the Southern Ocean (Carr et al. 2006).
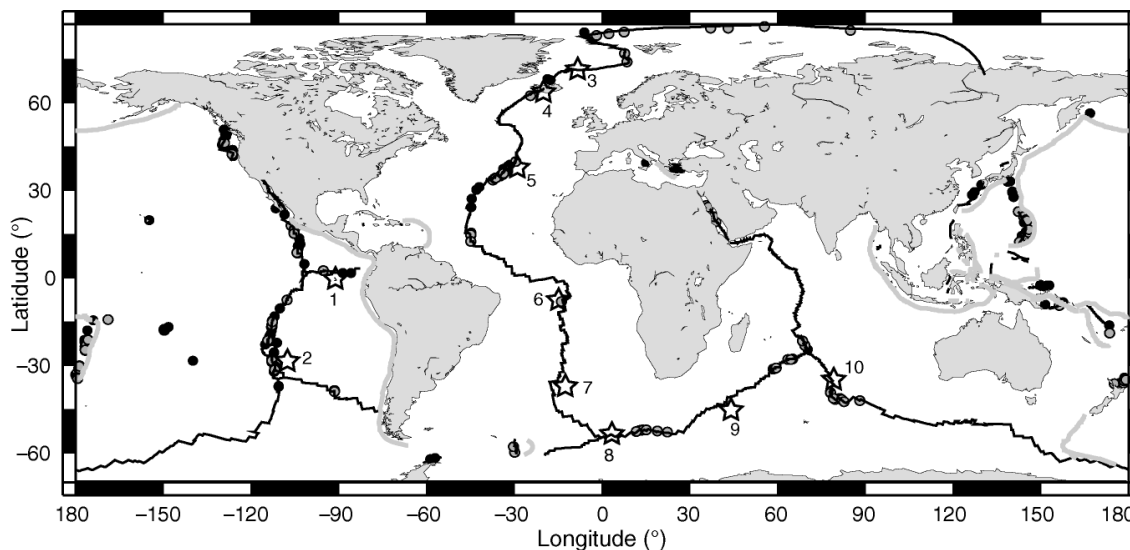
Figure 4: Known Hydrothermal Vent Locations

Figure 4 shows the distribution known hydrothermal vents along the mid-ocean ridge system. Of particular note is the distribution, or lack there of, in the Southern Ocean from paucity of data (Baker & German, 2004).

In 2015, Resing and co-workers detected elevated levels of Fe (in excess of 5nM) in a plume above the South Equatorial Pacific Rise between 2000-3000 m water depth caused by hydrothermal activity. What is interesting about this particular hydrothermal area is that the dFe behaved conservatively in the plume along the cruise track, rather than being scavenged and complexed out near the source. The discovery that dFe can behave conservatively when in a hydrothermal plume contradicts the long held view regarding hydrothermal contributions to deep-water dFe levels. The belief was that dFe quickly formed Fe-oxyhydroxides, which are quickly scavenged by biota or settled out (Feely et al. 1996).

As to why the dFe acts conservatively as it moves away from the hydrothermal vent, when it is expected that it should oxidize rapidly, Resing et al. (2015) offer some suggestions. They suggest that the dFe may be bound to organic ligands or may be in a colloidal form that does not settle out, as the particles are too small (Gerringa et al. 2008).

11

While Resing et al. (2015) suggest that more observational data is needed to confirm the

hypothesis, proposed not just by them; the data presented disproves the notion that

hydrothermal activity plays no role in the dFe budget of the ocean. The estimate is that

hydrothermal systems worldwide may contribute any where from 0-0.007 Tmol dFe yr^{-1}

(Figure 1). The estimate reflects the uncertainty of our understanding of these systems as

well as our ability to accurately sample them.

1.6 Trace Metal Sampling

Sampling ocean water for trace metals (TM) started in earnest in the 1970s out of

the desire to understand the distribution of the lower abundance elements in the ocean,

which was coupled with the technological advances that decreased detection limits of

analytical methods enabling the determination of these species. The GEOSECS

(Geochemical Ocean Sections Study) program of the 1970s provided the first concerted

sampling to describe large-scale distribution of chemical, isotopic, and radiochemical

tracers. The GEOSECS program spawned increased interest in what controlled TM

distribution in the ocean the knowledge of which then turned into a desire to use them to

understand biological and physical oceanic processes. Schaule and Patterson (1980,

1981) obtained the first non-contaminated Pb samples by using a single bottle sampler

attached to the end of a metallic hydrowire and closing the bottle on the down cast

thereby avoiding contamination of the sample by the metallic hydrowire. Bruland et al.

(1979) avoided the cable contamination problem by using a Dacron-sheathed, plastic

Phillystran hydrowire (Kevlar) with Teflon-coated 30-l PVC ball-valve samplers (GO-

FLO sampler, Figure 5) mounted on the cable.

Figure 5: GO-FLO Sampler

Figure 5: Picture of a Teflon-coated 30-l PVC ball-valve sampler courtesy of http://www.act-us.info.

The advantage in using GO-FLO samplers is that they come in a variety of sizes

for sample acquisition ranging from 1.7-100L. Boyle et al. (1986) was able to further

increase the efficiency of Pb sampling by obtaining multiple samples on a single

hydrocast by attaching a frame that freely rotates around the hydrowire containing a 250

mL polypropylene sampling bulb whose inlet would always be upstream of the

hydrowire. The Boyle et al. (1986) and Bruland et al. (1979) techniques allowed multiple

samples to be taken per cast this however requires stopping the cast and manually adding

or removing the bottles to/from the hydrowire. Additionally, with these systems the

bottles were triggered using a messenger that was dispatched from the surface once the

bottles were at the required depth, a process which could take over an hour to complete

for deep samples. While these were an improvement over the single sampling technique

of Patterson these two constraints still made the "bottles on a wire" techniques a slow,

cumbersome, and expensive method for obtaining TM samples.

A Trace metal clean rosette system (TMC) using a plastic-coated metal frame a

polyurethane-coated, three-conductor Kevlar hydroline and 8-mounted GO-FLO bottles

(Figure 6) was first developed by Hunter et al. (1996). The coatings on the frame and

hydroline proved effective in reducing metal contamination from the ctd components.

The TMC rosette-based system has now become the standard technique for TM sampling

in large-scale programs. International effort to map the distribution of trace elements in

the ocean using these rosette systems has made great progress in the last few decades.

The GEOTRACES and CLIVAR programs have started the process of mapping

biogeochemical distributions (Figures 7 & 8). The high-resolution sampling of the

CLIVAR program, 1° intervals, was designed to sample the top 1,000m, and thus does

not provide information on deep-sea TM signatures. The International GEOTRACES

program while at much lower resolution samples full depths at approximately half of its

stations providing insights into deep-water distributions and processes. As the previous

section demonstrates our collective understanding of the processes that TMs undergo is,

while nowhere near complete, somewhat well constrained, the distribution of TM's in the

ocean is lacking in spatial resolution, and for the most part is confined to the upper most

5,000m. The lack of data bellow 5,000m is partially a result of cost and limits of the

equipment used in the sampling methods.
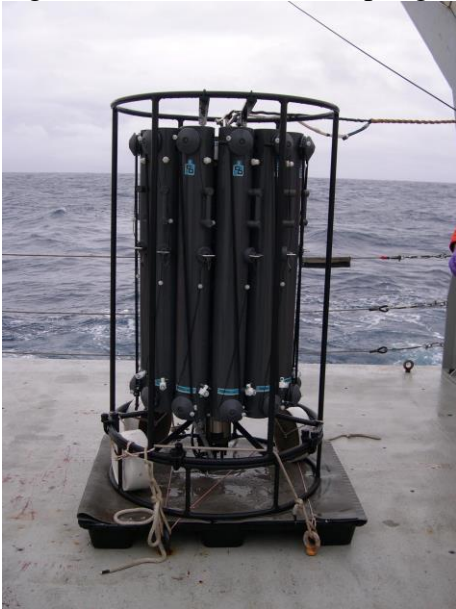
Figure 6: TMC Rosette Sampling System

Figure 6: Picture of a typical TMC rosette sampling system in wide use today.
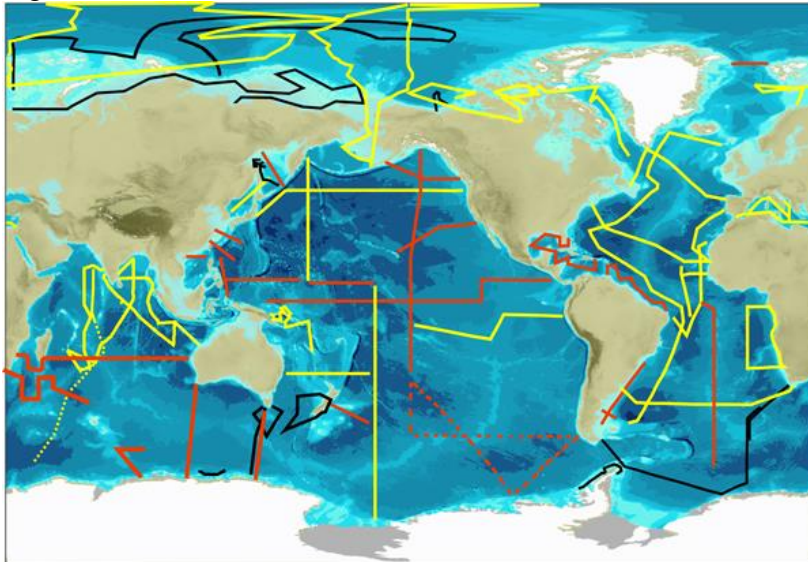
Figure 7: GEOTRACES Cruise Tracks

Figure 7: A map of the cruise tracks made by the GEOTRACES program. Courtesy of http://www.geotraces.org/.

Figure 8: CLIVAR Cruise Tracks

Figure 8: A map of the cruises tracks from the CLIVAR program.

While rosette systems have been highly effective and have assisted in mapping TM distributions, they are not without limitations. It is currently not possible to obtain water samples (TM clean or not) below 6,000m for several reasons. The first is that currently pressure cases for the ancillary instruments on the rosettes are limited to 6,000m. This design limitation is because the weight of the conventional metallic hydrowire used on normal rosettes exceeds its breaking strength if more than 6,000m is deployed, thus there little or no demand for greater pressure tolerance for the ancillary instruments. While the use of Kevlar hydrowire, which floats in water, eliminates this weight problem, the cost of Kevlar cable, and its thickness, requiring much larger winches, still limits the depths of sampling for economic reasons. Hadal regions, with depths of 10,000m or more are of increasing interest to the oceanographic community since there is little understanding of the physical processes that may ventilate these regions, or the biological communities that inhabit them or their geochemical status.

Since TM distributions can be proxies for a variety of physical and biological processes sampling for these parameters in the hadal regions could provide valuable information concerning the physical processes occurring within them and may also provide insight into their conditions during past climate conditions. The necessity to obtain water samples for this work has limited our ability to investigate these regions. Instead presented here is a method to obtain the concentration of trace metals in-situ, using on-line pre-concentration onto a column containing Toyopearl AF-Chelate-650m resin. This method, which has been developed using Fe can be extended to other trace elements. It is anticipated that the methodology could be attached to autonomous instruments which will allow for the sampling of previously inaccessible regions of the ocean for TM while increasing efficiency of current sampling efforts by decoupling TM sampling from the ship wire-time thus freeing up ship time for other sampling efforts.

2.0 METHODS

2.1 Pre-Concentration Method

The schematic for the pre-concentration system which consists of a bi-directional pump (milliGAT), a holding coil, a multi-position selection valve, and an external column packed with a resin is shown in Figure 9. The speed and volumes dispensed, within the system are fully computer controlled using commercially available software (FIAlab). Samples of water containing an Fe spike are passed through the resin column under a variety of conditions and aliquots of the effluent are collected to determine the dissolved Fe concentration using a flow injection analysis system (FIA, see below). By comparing the difference between the Fe concentration of the sample before passing through the resin column (Fe_s) and its concentration afterwards (Fe_f), the pre-concentration efficiency can be calculated.

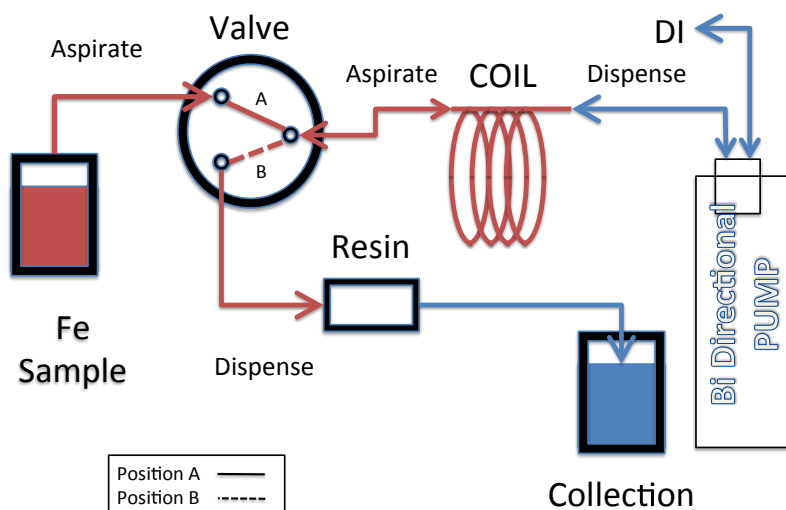Figure 9: Schematic Representation of the Pre-Concentration Method

Figure 9: Simplified representation illustrating the flow path of an Fe sample. The Fe Sample is aspirated through the valve filling the coil. Then dispensed back through the valve pre-concentrating on the resin as it flows to collection

2.1.1 Pre-Concentration Apparatus

The semi-automated system is controlled by the program FIAlab for Windows
version 5.11.10 and operated inside a flow bench as described below. The system consists
of the bi-directional milliGAT pump, which is used to fill a 14ml holding coil with a
deionized water (DI) sample that has been spiked with a known amount of Fe. After the
coil has been filled the valve is switched, the pump direction is reversed, and the sample
is dispensed through the resin column. An aliquot of the effluent, from the column, is
collected to determine its Fe content. The bi-directional pump is connected to a waste/DI
bottle on one side and a 1.55 mm internal diameter (ID) FEP (Up Church Scientific, Inc.
Cat# 1523) holding coil with a total volume of 14.9 mL on the other. The holding coil
connects to the main port of a multi-port selector valve (GlobalFIA, model: EMHMA-
CE). The selector valve connects to four parallel lines of 0.02" ID FEP tubing, each tube
holding a volume of 900µL. Three lines feed into Nalgene polypropylene bottles filled
with a cleaning solution (~0.5M HCL), DI, and the Fe_s sample while the fourth passes
through the resin column to waste/collection.

Prior to initial loading of the holding coil with a sample, and between samples the
acidic cleaning solution is aspirated into the holding coil, the valve position is switched
and the cleaning solution is dispensed through the resin line out to waste three times, this
removes any Fe residue from previous samples. After the acid rinsing then the system is
rinsed three times with DI water in the same manner. Before an Fe_s sample is aspirated
into the holding coil, DI is aspirated into the holding coil to act as a buffer between the
sample and pump. Following the DI solution, the Fe_s sample is aspirated in to the holding
coil. At this point the resin line contains 900µL of DI from the rinsing procedure, this

volume with an added 150μL (total 1050μL), to account for the mixing volume between the DI and Fe_s sample, is dispensed to waste. 4000μL of the Fe_s sample is then dispensed at 25μL s^{-1} across the resin and is collected as Fe_f sample by transferring the resin outlet tube to an acid cleaned bottle. The full FIAlab computer program is provided in the appendix.

To minimize airborne contaminants reagents and samples were contained within a class-100 laminar flow bench. All reagents used were the purest available and were exclusively prepared using ultra high purity DI with resistivity of >18.2 MΩ. Samples, standards, and reagents were contained in Nalgene polypropylene bottles and transferred using fluorinated ethylene propylene (FEP) tubing. All plastic ware was cleaned prior to use and between uses by leaching in ~0.5 M HCl, followed by rinsing three times with DI.

Pump Description:

MilliGAT^{TM} High Flow Bi-directional Pump (US Pat No. 6,079,313), Model No. CP-DSM2, serial No. EDSM05987. Maximum flow rate for the pump is 450μL s^{-1}.

Resin Description:

A number of resins were investigated for use in this project such as 8-hydroxyquinoline (8HQ), nitrilo-triacetate (NTA), and Nobias-chelate PA1 but were determined not suitable for this project based on a number of factors including cost and commercial availability. The resin chosen for use is Toyopearl AF-Chelate-650® resin (65 μm; Tosoh Bioscience LLC, #14475). This resin uses the functional group shown in Figure 10 and has been reported to be effective in extracting metals and rare earth

elements (Ndung'u et al. 2003, Zurbrick et al. 2013). The resin is shipped in an aqueous

solution by Tosoh Bioscience and was stored according to factory specifications. The

column was prepared by placing a filter on one end and injecting the resin, in the aqueous

solution, into the column until filled. The filter allows the aqueous solution to pass

through while the resin is immobilized in the column. Excess solution is removed by

passing DI through the resin. The resin is leached of contaminants by the soaking in

cleaning solution overnight followed by rinsing with DI.

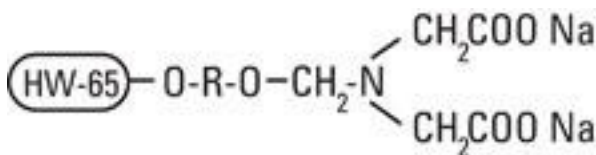Figure 10: Toyopearl Af-Chelate-650 Resin Functional Group

Figure 10: A depiction of the functional group, ligand density is 20μmol/mL for the Toyopearl AF-Chelate-650® resin. Courtesy of http://www.tosohbioscience.com/

Column description:

Commercially available columns, which are tapered, were found to cause

significant backpressure during initial flow rate testing. To overcome this obstacle a

custom made cylindrical column was manufactured specifically for this project by Global

FIA. The column has a uniform internal diameter of 2.54 mm with length 6mm, and an

internal volume of 30.4μL.

2.2 FIA Determination of Fe Concentrations

The concentration of dFe in the working standards and Fe_f samples was determined using a modified version of the flow injection analysis first described by Measures et al. (1995). Previous flow injection analytical work used a resin column to pre-concentrate samples in order to make the detection limit consistent with open ocean levels of dissolved Fe (Measures et al. 1995). For the dFe concentrations used in this work this was not necessary as the concentrations we were working with were much higher, instead we used a direct injection technique. The flow injection analysis (FIA) manifold used in this work is depicted in Figure 11. The apparatus consists of a 6-port injection valve operated by an electrically operated valve actuator under computer control. Flow is maintained at 7.5 rpm by an 8-channel peristaltic pump. All manifold tubing used is 0.02" internal diameter (ID) FEP (Up Church Scientific, Inc. Cat# 1548). The peristaltic pump tubing is flow rated PVC tubing (Fisher Scientific), with 0.76 ID for the sample, carrier and buffer lines, and 0.38mm ID for the H_2O_2 and DPD lines, displayed in Figure 11 to achieve the 0.3 and 0.05 mL/min desired flow rates consistent with Measures et al. (1995). All connections between tubing and valve or pump used acid cleaned flangeless ferrules (IDEX). Spectrophotometric detection is achieved by use of a Scientific Systems, INC. Model 500 Variable Wavelength Detector spectrophotometer set to measure absorbance at 514nm with rise time set to 3s. Peak detection from the spectrophotometer is done using Dynamax MacIntegrator DA 1 and R1 programs (Rainin Instruments, Inc.) running on an Apple Macintosh Powerbook model G3 computer, with further analysis on iMac PowerPC G4 using the program KaleidaGraph version 4.0 (Synergy Software).
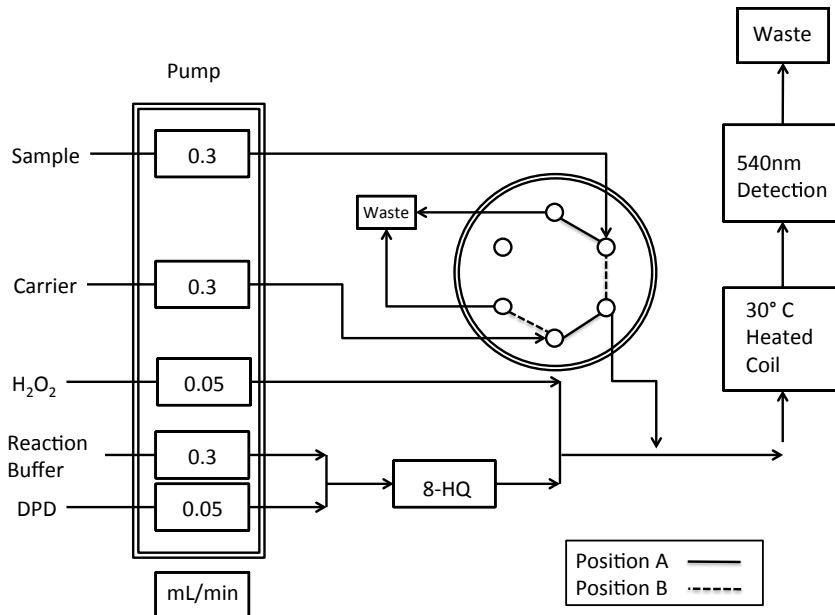
Figure 11: FIA Schematic

Figure 11: Depiction of the FIA schematic used to analyze Fe standards and samples. Flow rates for reagents are displayed in the pump box.

This method allows for automated controls of the 6-port injection valve for precise sample injection times. A single column of 8-hydroxyquinoline (8HQ) immobilized on vinyl polymer gel is immersed in ice and used to remove contaminants from N,N-dimethyl-p-phenylenediamine (4-amino-N, N-dimethylaniline) dihydrocloride (DPD) as well as to allow the catalytic reaction between the reaction buffer and DPD to slow. Once the DPD, H_2O_2, and reaction buffer are combined with either carrier/sample/standard the mixture flows through a heating coil bringing the temperature of the reaction up to 30° C.

2.2.1 On-Line Setup

The 6-port injection valve is used to switch the system from the Fe carrier to working standard/Fe$_f$ sample, while one line is supplying the spectrophotometer the other

flows to waste. During the course of the experiments it was found that during the switch between the supply lines the flow is interrupted due to backpressure in the system, this interruption results in a pre-peak and a slight increase in the baseline absorbance. To avoid this problem peak height measurements for the sample were made relative to the baseline established when the carrier was flowing through the sample line.

This was accomplished as follows. An initial baseline is established using the Fe carrier flowing through the sample line, the valve is then switched to the carrier line and the sample line is moved to the standard/sample container. This transfer introduces an air bubble into the system, so the system is left pumping for two minutes to let the air bubble pass to waste. After two minutes, the valve is switched from the carrier line back to the sample line with standard/Fe_f sample flowing for 30s, after which the valve switches back to the carrier line. The sample line is then transferred back to the Fe carrier solution. Two minutes are allowed to pass, and then the valve is switched back to the sample line position and the process is repeated. Triplicate determinations were made to assess the precision of the system, with a five-minute interval between each sample injection. A typical detector output from spectrophotometric analysis of an Fe sample is shown in Figure 12.

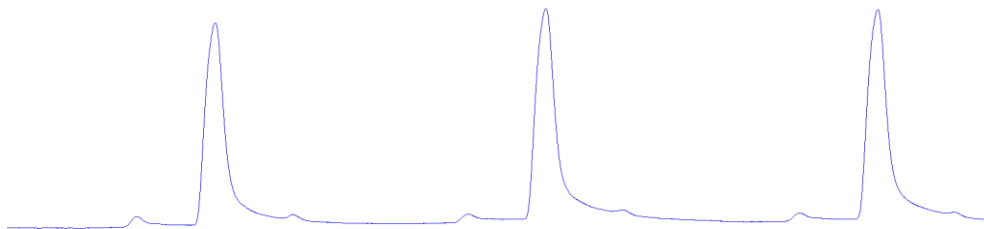Figure 12: Detector Output of Spectrophotometer

Figure 12: Typical detector output from the spectrophotometer. Y-axis is in arbitrary absorbance units and the x-axis is time. The standard being measured in triplicate here is for a 13.93 nM Fe standard.

2.3 Reagents

      2.3.1 Reagents for the Pre-Concentration System

Eluant:

      Hydrochloric acid (HCl, 6M) is prepared using trace metal grade (TMG) HCl in a

quartz-finger, sub-boiling distillation apparatus. The eluant, which is also used as a

cleaning solution to flush the system between experiments, is made by diluting 24mL

HCl with 1L DI.

Fe$_s$ Sample:

      A secondary standard with [Fe] 35.6µM was prepared as needed by serial

dilutions of a 17.9mM Fe primary standard (Fisher Scientific) using acidified DI

containing and 4mL sub-boiled 6M HCl/L of DI. Fe$_s$ samples were prepared daily by

dilution of the 35.6µM secondary standard into DI until the desired concentrations of

~14.2, ~7.1, ~3.55, and ~0.5nM Fe were achieved (accurate concentrations were

determined for individual days). A 100 mL volume of each Fe$_s$ sample was prepared

daily with 50mL allocated for use as the working standard for the FIA method while the

remaining 50mL was used as the Fe$_s$ sample used for the pre-concentration experiments.

The FIA working standard was acidified with 1.2mL HCl, the 50 mL Fe$_s$ sample was left

unacidified

2.3.2 Reagents for the FIA Determination

Fe Carrier:

The Fe carrier was prepared by adding 24mL of sub-boiled 6M HCl to 1L DI.

DPD:

N,N-dimethyl-p-phenylenediamine (4-amino-N, N-dimethylaniline) dihydrocloride (0.046M) was prepared daily by dissolving 1 g DPD in 100mL of DI containing 400μL of 6M HCl.

H_2O_2:

H_2O_2 (5%) was prepared as needed by diluting 42mL 30% H_2O_2 (Sigma-Aldrich) with DI to 252mL.

Reaction Buffer:

Ammonium acetate buffer (2M) was prepared by adding 115mL of sub-boiled acetic acid to 1.76mol of trace metal grade NH_4OH (Measures et al. 1995). The mix is diluted with DI to 1L with a resulting pH of 6.3±0.1.

Working Standard:

Working standards are prepared daily as described above, the 50mL set aside for FIA determination is combined with 1.2mL 6M HCl to bring the standard pH to that of the carrier (pH = 0.85).

Fe$_f$ Sample:

The sample is collected from the outlet of the resin column into a pre-weighed bottle and weighed after the collection process is complete to determine sample weight. Using this weight the sample pH is then adjusted to that of the carrier (pH = 0.85) by the addition of the appropriate amount of 6M HCL.

3.0 RESULTS AND DISCUSSION

3.1 Results Overview

The goal of this thesis was to develop a simple pre-concentration technique using a resin column and milliGAT pump that could remove dFe from DI water. In this section I will discuss the optimization of the pre-concentration system (Section 3.2) and the capacity of the resin (Section 3.3).

3.2 Optimizing Pre-Concentration System

3.2.1 Elimination of Fe Contamination from the Pump

Since the concentration of trace metals in seawater is extremely low and because samples are easily contaminated during the sampling procedure, it is important to eliminate any contamination from this system (individual components, especially the milliGAT pump). Indeed, it had previously been observed that solutions passing through the milliGAT pump were observed to have higher dFe levels. The materials used in the milliGAT pump are difficult to clean using our trace metal cleaning procedure. Thus, any solution that contacts the pumphead is likely to be contaminated. Therefore, our pre-concentration system (Figure 9) was designed to prevent any of the sample that has come directly into contact with the milliGAT pumphead from being passed through the resin column. In the laboratory this was achieved by initially filling the coil with DI water prior to aspirating the sample into the coil. At this point the pump is reversed and the sample is dispensed through the resin column. However, the DI water that has contacted

the milliGAT pumphead will mix with the sample solution in the coil that has not passed

through the pumphead. Thus, it was necessary to determine the extent of the mixing zone

between the solution that has contacted the pumphead and the sample that had been

drawn into the coil. To investigate this the equipment was modified by adding a

spectrophotometer on the waste side of the pump (Figure 13).

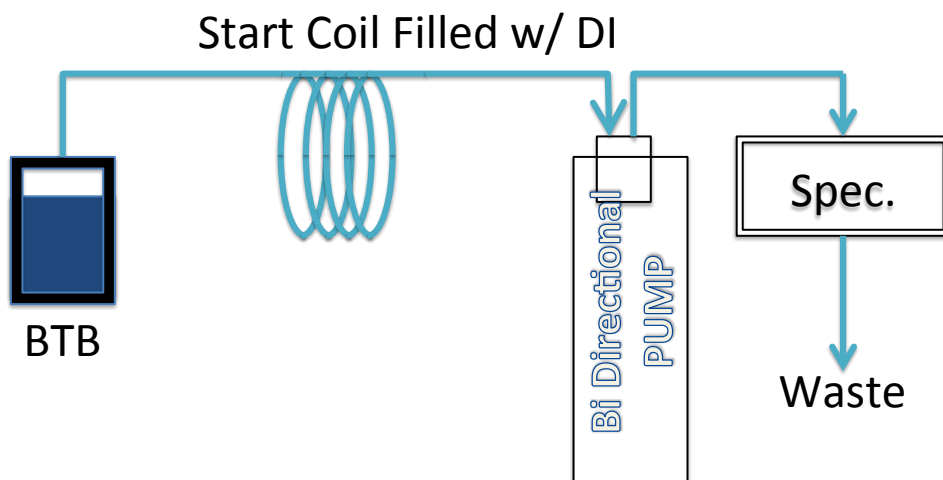Figure 13: Modified Pump System with Spectrophotometer

Figure 13: Depiction of the modified pump system used to determine contamination from the pump. The coil starts filled with acidified DI, and then BTB is aspirated into the coil pushing the DI through the spectrophotometer where absorbance is measured.

The extent of the mixing zone was determined by aspirating an acidified DI water sample

into the coil (representing the Fe_s sample) and this was followed by a solution of

Bromothymol blue (BTB) representing the solution that had contacted the pumphead.

Since the blue BTB solution changes color to yellow when the solution is mixed with

acid, the mixing zone can be visually identified by monitoring absorbance at 470 nm with

the spectrophotometer. A typical transition is displayed in Figure 14 and from the time of

the appearance of the mixing zone the volume of the uncontaminated sample that could be delivered to the resin column can be calculated. The results showed that ~10.5mL of the 14.9mL coil volume could be delivered before the appearance of the mixing zone. This volume represents ~70% of the total volume. The dispensing velocity appeared to have no effect as the volume of "non-contaminated" sample solution remained constant using flow rates of 50-to-100-μL s^{-1} (Fig 15)

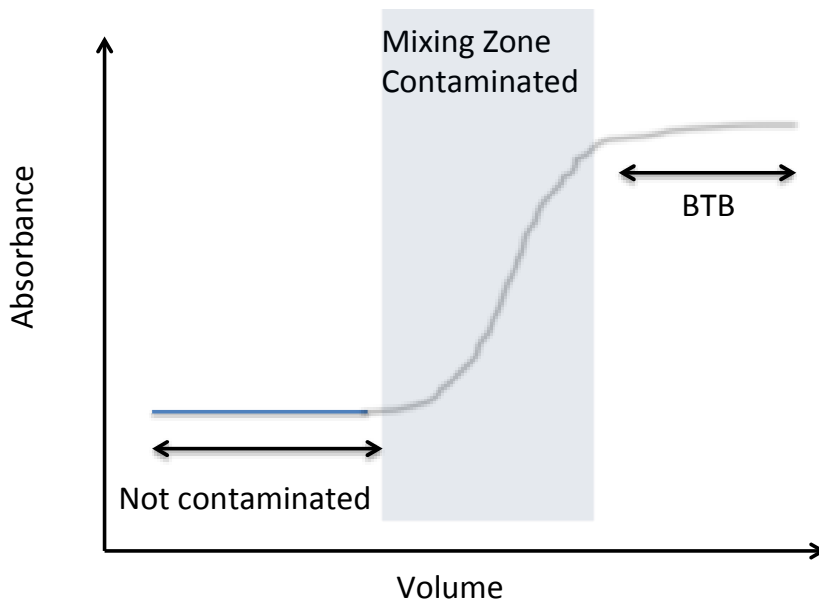Figure 14: Typical Detector Output from Contamination Testing

Figure 14: display of the typical detector output from contamination testing. Deviation from the original baseline represents arrival of contamination from the pump (yellow). The x-axis is volume and y-axis is in arbitrary absorbance units. Courtesy Dr. Mariko Hatta

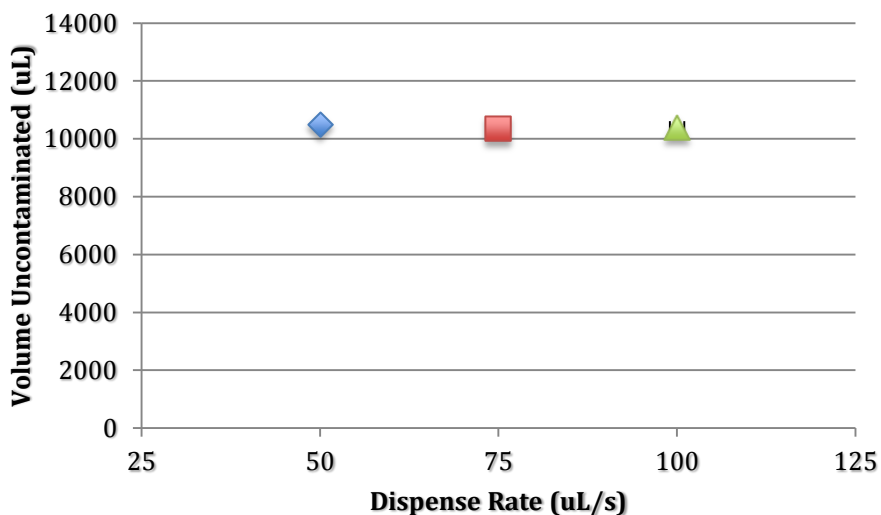Figure 15: Volume of Solution Uncontaminated by Pump

Figure 15: The volume of solution not subject to contamination from the pump. N=3 and standard deviations are plotted but are difficult to be seen as they are 2, 3, and 2.3% for the dispense rates of 50, 75, and 100 μL/s respectively.

3.2.2 Optimizing the Flow Rate of the Pre-Concentration System

In order to accurately determine the amount of Fe pre-concentrated onto the resin in-situ, it is important to know the volume of the sample passing through the resin column. The Toyopearl resin used in the pre-concentration system (depicted in Figure 9) introduces backpressure into the system, resulting in a smaller volume passing through the resin than has been programmed. To evaluate this the pump was programmed to dispense 4000μL of DI across the resin at different flow rates and the actual dispensed volume was measured gravimetrically. The results showed that the milliGAT pump had aspirated/dispensed a volume that was less than had been programmed (Table 1). It was found that as the flow rates were increased, backpressure increased and a smaller volume passed through the resin (Table 1; Figure 16), Thus we chose a rate of $25 \mu Ls^{-1}$ as it was closest to the desired volume.

Table 1: Actual Dispensed Volume as a Function of Flow Rate

Rate (uL/s)	Desired Vol. (uL)	Avg. Actual Vol. (uL)	Std. (uL)
25	4000	3816	28.87
50	4000	3703	29.67
75	4000	3636	2.01

Table 1: How actual dispensed volume varies with flow rate due to increased back pressure from the in-line resin column, n=3.

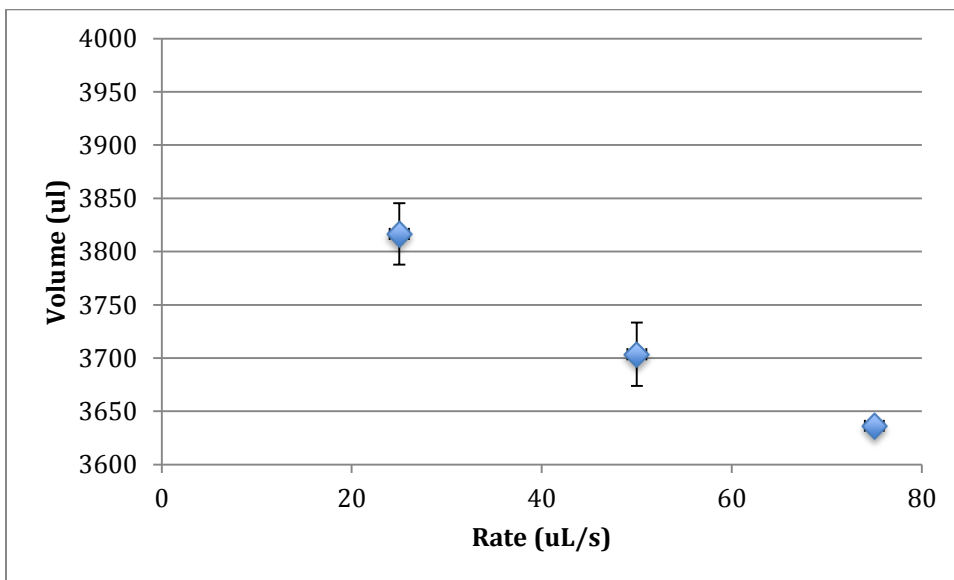Figure 16: Actual Volume Dispensed Relative to a Nominal of 4000μL as a Function of Pumping Rate

Figure 16: Volume dispensed as a function of flow rate relative to a Nominal 4000μL volume (N=3). The largest standard deviation of the replicates was ±30μL or <1%.

3.3 Capability of the Pre-Concentration Method

3.3.1 FIA Parameters

In order to obtain the Fe concentration before/after the developed pre-concentration system, a simple FIA system for Fe determination was set up (Figure 11). Peak heights were measured by dropping a perpendicular from the peak apex to the baseline established by running the carrier through the sample line (see section 2.2.2).

These peak heights were corrected by the amount of the baseline disturbance that underlies the Fe peak as a result of the valve switch temporarily changing the flow rate of the carrier. The value for this correction was obtained by switching the valve when both lines were in the carrier and measuring the resulting peaks. The value of the pre-peak was found to be 11,296 AU $+$ 977 (n=3), approximately 1 ± 0.1nM. The detection limit for analysis using the FIA system was estimated by measuring the standard deviation of the peak heights of three different Fe_s samples in triplicate and multiplying the standard deviation by three (Table 2). The largest of the three standard deviations was from the 6.91nM standard was used to calculate the detection limit. That value, when multiplied by three was 3645AU, which implies a detection limit of 0.355nM.

The standard curve was produced from the three working standards (Table 2) and a regression line was fit through the average of each of the standards the correlation coefficient (R^2) was 0.9997 (Figure 17).

Table 2: Working Standard Concentrations with Absorbance

Standard Conc. (nM Fe)	Absorbance (AU)	Std. (AU)
3.34	36988	230
6.91	73245	1215
13.93	147788	1165

Table 2: Working standard concentrations in nM Fe with the corresponding absorbance readings and standard deviations from the spectrophotometer, n=3.

3.3.2 Fe_f Sample Determination

The concentration of dissolved Fe in the Fe_f samples which were produced by dispensing a standard through the Toyopearl AF-Chelate-650® resin was determined using the FIA method (described above). The difference between the initial concentration of dissolved Fe in the acidified standard (Fe_s) and the Fe_f sample is equal to the amount of dissolved Fe absorbed by the resin (Fe_a; 2).

(2) $[Fe]_a = [Fe]_s - [Fe]_f$

Fe_f sample concentrations were determined, after correction, using the equation of the standard curve. The results showed that for working standards with concentrations ranging from 3.34-13.93nM passed through the resin column at 25ul/s the concentration of dissolved Fe was below the detection limit of the system (355nM; Figure 18). Based on the highest concentration standard (13.93 nM), this implies that the resin adsorbed at least 97.47% ± 0.82% of the Fe. This also implies that this Toyopearl Af-Chelate-650resin column had a capacity of at least 446.71 ± 3.76 μmol Fe L^{-1} of resin.
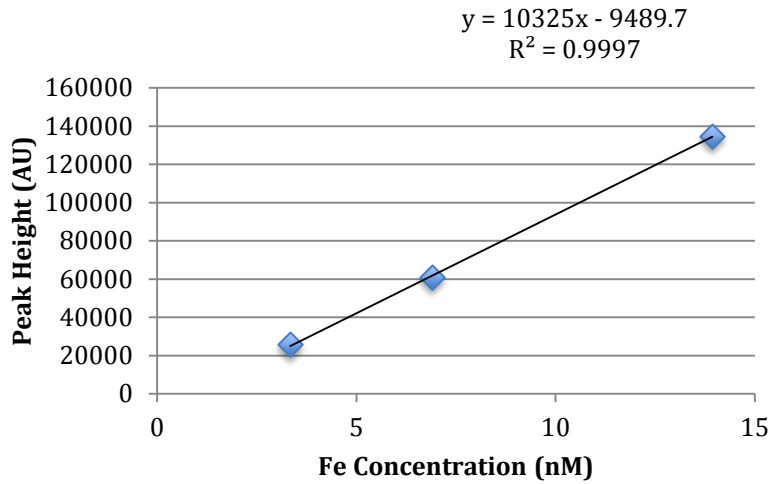
Figure 17: Standard Curve

Figure 17: Standard curve for the working standards with concentrations of ~3.34, 6.91, and 13.93 nM (n=3). The linear regression equation is displayed along with the R^2 coefficient.

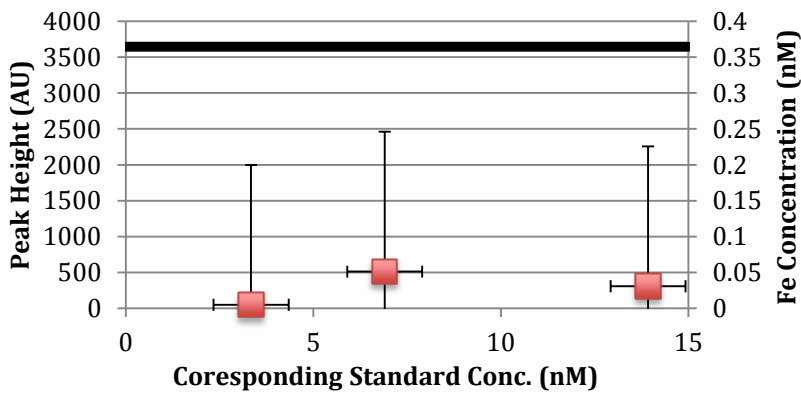Figure 18: Fe_f Sample Peak Heights (w/ Detection Limit)

Figure 18: The average Fe_f sample peak heights (n=3) corresponding to Fe_s sample of ~3.34, 6.91, 13.93 are displayed along with the standard deviation. The detection limit is displayed as a black line; all samples fell below the detection limit. A secondary y-axis is displayed with the calculated Fe concentration from the standard curve linear regression

3.4 Future Work

As mentioned this is the first stage of development on a large project with the goal of developing a resin-column based system that could be placed on autonomous underwater vehicles, remotely operated underwater vehicles, or other such systems to pre-concentrate trace elements from seawater. Such a system could be designed to be part of a cartridge system that can be easily interchanged on a package (Figure 19). The pre-concentrated materials could be released in a shore based analytical laboratory saving millions of dollars and thousands of hours of ship time in sample acquisition, which as it currently stands is both labor and time intensive. Further stages of development include expansion of elements for pre-concentration, of which a large body of work already exists, along with further confirmation of the findings by means of HR ICP-MS (Ndung'u et al. 2003, Zurbrick et al. 2013). Implementation of this technique on a near shore buoy for environmental monitoring will be the subject of my Masters Thesis. Further, tethered, shipboard open ocean tests will be made once near shore testing is complete. Ultimately, this method could see widespread adoption on the ARGO program, research cruises, and eventually on a hadal lander (Figure 20) to probe the recesses of the hadal region.
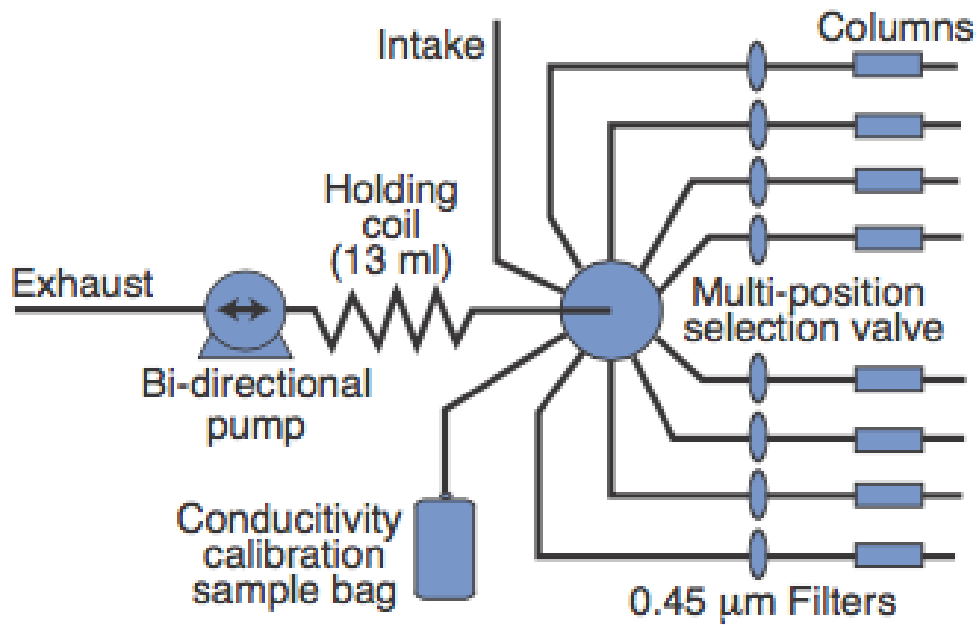
Figure 19: Concept for Final Wet Chemistry

Figure 19: Schematic for the final design of the replaceable cartridge based system. Courtesy Dr. Chis Measures.

Figure 20: VMP Profiler

Figure 20: An example of an autonomous system that could be adapted to utilize the pre-concentration method described in this thesis. Courtesy Dr. Carter.

4.0 CONCLUSION

From measurements of Fe_s samples before and after pre-concentration on a resin column, it was found that any Fe present in the sample was successfully adsorbed to the resin. The rate chosen for passing the Fe_s samples over the resin is $25\mu L\ s^{-1}$. Contamination from the pumping mechanism to an Fe_s sample is limited to 30% of the total volume of the holding coil. The pre-concentration efficiency of the resin is 97.47% $\pm\ 0.82\%$, and the maximum capacity of the resin measured during experimentation is $446.71 \pm 3.76\mu mol\ Fe\ L^{-1}$. Based off of the findings presented here the next stage in development of this method will begin in earnest in the Fall of 2016.

APPENDIX

FIA Computer Controls

Loop Start (#) 3
InjLoad_Valve port 2
Multiposition Valve Acid
Milligat1_HF Flowrate (microliter/sec) 50
Milligat1_HF Dispense (microliter) 7550
Milligat1_HF Delay Until Done

Multiposition Valve Column
Milligat1_HF Flowrate (microliter/sec) 50
Milligat1_HF Aspirate (microliter) 7550
Milligat1_HF Delay Until Done
Loop End

Loop Start (#) 3
Multiposition Valve DI
Milligat1_HF Flowrate (microliter/sec) 50
Milligat1_HF Dispense (microliter) 7550
Milligat1_HF Delay Until Done

Multiposition Valve Column
Milligat1_HF Flowrate (microliter/sec) 50
Milligat1_HF Aspirate (microliter) 7550
Milligat1_HF Delay Until Done
Loop End

Multiposition Valve DI
Milligat1_HF Flowrate (microliter/sec) 50
Milligat1_HF Dispense (microliter) 2000
Milligat1_HF Delay Until Done

Multiposition Valve Sample
Milligat1_HF Flowrate (microliter/sec) 50
Milligat1_HF Dispense (microliter) 6550
Milligat1_HF Delay Until Done

Multiposition Valve Column
Milligat1_HF Flowrate (microliter/sec) 50
Milligat1_HF Aspirate (microliter) 1050
Milligat1_HF Delay Until Done

Multiposition Valve Column
Milligat1_HF Flowrate (microliter/sec) 25
Milligat1_HF Aspirate (microliter) 4000
Milligat1_HF Delay Until Done

LITERATURE CITED

Antoine, D., Andre, J. M., & Morel, A. (1996). Oceanic primary production .2. Estimation at global scale from satellite (coastal zone color scanner) chlorophyll. *Global Biogeochemical Cycles, 10*(1), 57-69. doi:10.1029/95gb02832

Baker, E. T., & German, C. R. (2004). On the global distribution of hydrothermal vent fields. *Mid-ocean ridges: hydrothermal interactions between the lithosphere and oceans*, *148*, 245-266.

Bowman, K. P., & Cohen, P. J. (1997). Interhemispheric exchange by seasonal modulation of the Hadley circulation. *Journal of the atmospheric sciences*, *54*(16), 2045-2059. (Bowman & Cohen, 1997)

Boyle, E. A., Chapnick, S. D., Shen, G. T., & Bacon, M. P. (1986). Temporal variability of lead in the western North Atlantic. *Journal of Geophysical Research: Oceans*, *91*(C7), 8573-8593.

Bruland, K. W., R. P. Franks, G. A. Knauer, and J. H. Martin. 1979. Sampling and analytical methods for the determination of copper, cadmium, zinc, and nickel at the nanogram per liter level in sea water. Anal. Chim. Acta 105:233-245.

Carr, M. E., Friedrichs, M. A., Schmeltz, M., Aita, M. N., Antoine, D., Arrigo, K. R., & Yamanaka, Y. (2006). A comparison of global estimates of marine primary production from ocean color. *Deep Sea Research Part II: Topical Studies in Oceanography*, *53*(5), 741-770.

Duce, R. A., & Tindale, N. W. (1991). Atmospheric Transport Of Iron And Its

    Deposition In The Ocean. *Limnology and Oceanography, 36*(8), 1715-1726.

Fantle, M. S., & DePaolo, D. J. (2004). Iron isotopic fractionation during continental

    weathering. *Earth and Planetary Science Letters, 228*(3-4), 547-   562.

    doi:10.1016/j.epsl.2004.10.013

Feely, R. A., Baker, E. T., Marumo, K., Urabe, T., Ishibashi, J., Gendron, J., ... &

    Okamura, K. (1996). Hydrothermal plume particles and dissolved phosphate over

    the superfast-spreading southern East Pacific Rise. *Geochimica et   Cosmochimica*

    Acta, *60*(13), 2297-2323.

Georgiadis, M. M., Komiya, H., Chakrabarti, P., Woo, D., Kornuc, J. J., & Rees, D. C.

    (1992). Crystallographic structure of the nitrogenase iron protein from

    Azotobacter vinelandii. *Science*, *257*(5077), 1653-1659.

Gerringa, L. J., Blain, S., Laan, P., Sarthou, G., Veldhuis, M. J. W., Brussaard, C. P. D.,

    & Timmermans, K. R. (2008). Fe-binding dissolved organic ligands near the

    Kerguelen Archipelago in the Southern Ocean (Indian sector). *Deep Sea Research*

    Part II: Topical Studies in Oceanography, *55*(5), 606-621.

Gris, E. "Nouvelles experiences sur l'action des composes ferrugineux soulubiles,

    appliques a la vegetation, et specialement au traitement de la chlorose et de la

    debilite des plantes." Comp. Rend Acad. Sci (paris) 19:1118-1119. 1844

Haase, K. M., Petersen, S., Koschinsky, A., Seifert, R., Devey, C. W., Keir, R., ... &

    Weber, S. (2007). Young volcanism and related hydrothermal activity at 5 S on

    the slow‐ spreading southern Mid‐ Atlantic Ridge. *Geochemistry, Geophysics,*

    Geosystems, *8*(11).

Hunter, C. N., Gordon, R. M., Fitzwater, S. E., & Coale, K. H. (1996). A rosette system for the collection of trace metal clean seawater. *Limnology and Oceanography*, *41*(6), 1367-1372.

J.H. Martin, K.H. Coale, K.S. Johnson, S.E. Fitzwater, R.M. Gordon, S.J. Tanner, C.N. Hunter, V.A. Elrod, J.L. Nowicki, T.L. Coley, R.T. Barber, S. Lindley, A.J. Watson, K. Van Scoy, C.S. Law, M.I. Liddicoat, R. Ling, T. Stanton, J. Stockel, C. Collins, A. Anderson, R. Bidigare, M. Ondrusek, M. Latasa, F.J. Millero, K. Lee, W. Yao, J.Z. Zhang, G. Friederich, C. Sakamoto, F. Chavez, K. Buck, Z. Kolber, R. Greene, P. Falkowski, S.W. Chisholm, F. Hoge, R. Swift, J. Yungel, S. Turner, P. Nightingale, A. Hatton, P. Liss, N.W. Tindale Testing the iron hypothesis in ecosystems of the equatorial Pacific Ocean Nature, 371 (1994), pp. 123–129

Jickells TD, Spokes LJ. In: Turner DR, Hunter KA, eds. The Biogeochemistry of Iron in Seawater. Chichester, West Sussex: John Wiley & Sons, 2001:85 – 121.

Jickells, T. D., An, Z. S., Andersen, K. K., Baker, A. R., Bergametti, G., Brooks, N., Torres, R. (2005). Global iron connections between desert dust, ocean biogeochemistry, and climate. *Science, 308*(5718), 67-71 .doi:10.1126/science.1105959

Mahowald, N. M., Baker, A. R., Bergametti, G., Brooks, N., Duce, R. A., Jickells, T. D., Tegen, I. (2005). Atmospheric global dust cycle and iron inputs to the ocean. *Global Biogeochemical Cycles, 19*(4), 17. doi:10.1029/2004gb002402

Martin, J. H., & Gordon, R. M. (1988). Northeast Pacific iron distributions in relation to

    phytoplankton productivity. *Deep Sea Research Part A. Oceanographic Research*

    Papers, *35*(2), 177-196.

Measures, C. I., Landing, W. M., Brown, M. T., & Buck, C. S. (2008). High-resolution

    Al and Fe data from the Atlantic Ocean CLIVAR-CO(2) repeat hydrography

    A16N transect: Extensive linkages between atmospheric dust and upper ocean

    geochemistry. *Global Biogeochemical Cycles, 22*(1), 10.

    doi:10.1029/2007gb003042

Measures, C. I., Yuan, J., & Resing, J. A. (1995). Determination of iron in seawater by

    flow injection analysis using in-line preconcentration and spectrophotometric

    detection. *Marine chemistry*, *50*(1), 3-12.

Morales, C. (1986). The airborne transport of Saharan dust: a review. *Climatic*

    Change, *9*(1-2), 219-241.

Morgan, J. W., & Anders, E. (1980). Chemical composition of Earth, Venus, and

    Mercury. *Proceedings of the National Academy of Sciences of the United States of*

    America, *77*(12), 6973–6977.

Ndung'u, K., Franks, R. P., Bruland, K. W., & Flegal, A. R. (2003). Organic

    complexation and total dissolved trace metal analysis in estuarine waters:

    comparison of solvent-extraction graphite furnace atomic absorption

    spectrometric and chelating resin flow injection inductively coupled plasma-mass

    spectrometric analysis. *Analytica Chimica Acta*, *481*(1), 127-138.

Prospero, J. M., P. Ginoux, O. Torres, S. E. Nicholson, and T. E. Gill, Environmental

    Characterization Of Global Sources Of Atmospheric Soil DUST Identified With

The Nimbus 7 Total Ozone Mapping Spectrometer (Toms) Absorbing Aerosol
Product, Rev. Geophys., 40(1), 1002, doi:doi:10.1029/2000RG000095, 2002.

R. A. Duce, in *Aerosol Forcing of Climate*, R. J. Charlson, J. Heintzenberger, Eds.
(Wiley, Chichester, UK, 1995), pp. 43–72.

Raven, John A., Michael CW Evans, and Rebecca E. Korb. "The role of trace metals in
photosynthetic electron transport in O2-evolving organisms."*Photosynthesis
Research* 60.2-3 (1999): 111-150.

Resing, J. A., Sedwick, P. N., German, C. R., Jenkins, W. J., Moffett, J. W., Sohst, B. M.,
& Tagliabue, A. (2015). Basin-scale transport of hydrothermal dissolved metals
across the South Pacific Ocean. *Nature*, *523*(7559), 200-203.

Schaule, B. K., and C. C. Patterson. 1980. The occurrence of Lead in the Northeast
Pacific and the effects of Anthropogenic Inputs. In: M. Branica and Z. Konrad,
Eds. Lead in the Marine Environment. Oxford: Pergamon Press, p. 31- 43.

Schaule, B. K., and C.C. Patterson. 1981. Lead concentration in the Northeast Pacific:
evidence for global anthropogenic perturbations. Earth Planet. Sci. Lett. 54:97-
116.

Schlesinger WH, Bernhardt ES (2013) Biogeochemistry: An Analysis of Global Change,
3rd edn. Academic Press/Elsevier, Amsterdam . pp. 74-75

Spokes, L. J., & Jickells, T. D. (1995). Factors controlling the solubility of aerosol trace
metals in the atmosphere and on mixing into seawater. *Aquatic
Geochemistry*, *1*(4), 355-374.

Street, J. H., & Paytan, A. (2005). Iron, phytoplankton growth, and the carbon cycle. *Met
Ions Biol Syst*, *43*, 153-93.

Sugden, D. E., McCulloch, R. D., Bory, A. J. M., & Hein, A. S. (2009). Influence of

    Patagonian glaciers on Antarctic dust deposition during the last glacial

    period. *Nature Geoscience*, *2*(4), 281-285.

Sunda, William G., Dorothy G. Swift, and Susan A. Huntsman. "Low iron requirement

    for growth in oceanic phytoplankton." (1991): 55-57.

Weeks, D. A., & Bruland, K. W. (2002). Improved method for shipboard   determination

    of iron in seawater by flow injection analysis. *Analytica Chimica Acta*, *453*(1),

    21-32.

Westphal, D. L., Toon, O. B., & Carlson, T. N. (1987). A two-dimensional numerical

    investigation of the dynamics and microphysics of Saharan dust storms. Journal of

    Geophysical Research: Atmospheres, 92(D3), 3027-3049.

Yücel, M., Gartman, A., Chan, C. S., & Luther III, G. W. (2011). Hydrothermal vents as

    a kinetically stable source of iron-sulphide-bearing nanoparticles to the

    ocean. *Nature Geoscience*, *4*(6), 367-371.

Zurbrick, C. M., Gallon, C., & Flegal, A. R. (2013). A new method for stable lead isotope

    extraction from seawater. *Analytica chimica acta*, *800*, 29-35.